conformation as that of the *D* ring in 2β,3α-dichloro-5α-cholestane, in which the *A* ring is normal, and in which there is no bromine atom attached to the *C* ring (Geise, Romers & Rutten, 1966). The packing of the molecules in the two cases is quite different. In the case of the 12α-bromo derivative, the bulky bromine group on the α-surface causes a fairly large intermolecular separation. This loosened packing arrangement allows a comparatively free rotation of the side chain about the C(17)–C(20) bond, resulting in the unusual side chain orientation observed in this molecule. The more compact packing arrangement achieved in the 12β-bromo derivative causes the side chain to take up the more frequently observed 'extended' conformation.

References

BONHAM, R. A. & BARTELL, L. S. (1959). *J. Amer. Chem. Soc.* **81**, 3491.
GEISE, H. J., ROMERS, C. & RUTTEN, E. W. M. (1966). *Acta Cryst.* **20**, 249.
GOPALAKRISHNA, E. M., COOPER, A. & NORTON, D. A. (1969). *Acta Cryst.* B25, 143.
International Tables for X-ray Crystallography (1962). Vol. III. Birmingham: Kynoch Press.
KLYNE, W. & PRELOG, V. (1960). *Experientia*, **16**, 521.
MATTOX, V. R., TURNER, R. B., ENGEL, L. L., MCKENZIE, B. F., MCGUCKIN, W. F. & KENDALL, E. C. (1946). *J. Biol. Chem.* **164**, 599, 582, 590.
MATTOX, V. R., TURNER, R. B., ENGEL, L. L., MCKENZIE, B. F., MCGUCKIN, W. F. & KENDALL, E. C. (1948). *J. Biol. Chem.* **173**, 283, 286, 290.
WILSON, A. J. C. (1942). *Nature, Lond.* **150**, 151.

The Crystal and Molecular Structure of Hypoxanthine Hydrochloride Monohydrate

BY JORUNN SLETTEN AND LYLE H. JENSEN

Department of Biological Structure, University of Washington, Seattle, Washington, U.S.A.

The structure of hypoxanthine hydrochloride monohydrate, [C$_5$N$_4$H$_5$O]Cl.H$_2$O, has been solved by X-ray crystallographic methods. The crystals are monoclinic, space group P2$_1$/c, with $a=4\cdot8295$ Å, $b=17\cdot7285$ Å, $c=9\cdot0077$ Å and $\beta=94\cdot59°$ ($t=20°\pm2°$C). 1769 reflections were measured on a manually operated diffractometer with Mo Kα radiation. The structure was refined to $R=0\cdot030$. Standard deviations in bond lengths and angles involving nonhydrogen atoms are in the range 0·0014–0·0018 Å and 0·03–0·07° respectively. The hypoxanthine cation is present in the lactam form and the nitrogen atoms N(1), N(7) and N(9) carry hydrogen atoms. The molecules are linked together through extensive hydrogen bonding. The spacing between layers of molecules is 3·18 Å, and there is virtually no overlap between molecules in adjacent layers.

Introduction

The hypoxanthine nucleotide inosinic acid is the first purine compound formed in the biosynthesis of purine nucleotides, and it is the precursor of both adenylic and guanylic acid. Any structure which is an antagonist for hypoxanthine will block nucleic acid synthesis. The structure of one such antagonist, 6-mercaptopurine, has already been determined (Sletten, Sletten & Jensen, 1969), and it is important to establish dimensional similarities and differences between this structure and hypoxanthine. The present paper is a report of the structure of the monohydrate of hypoxanthine hydrochloride.

Experimental

Hypoxanthine was obtained from Sigma Chemical Company, St. Louis, Missouri, and crystals of hypoxanthine hydrochloride were grown from a 1N HCl solution by slow evaporation.

Cell parameters were determined by least-squares treatment of the 2θ settings for 14 reflections as measured on the diffractometer. The mean deviation between the observed and computed 2θ values, 1/14 ($\Sigma |2\theta_{obs}-2\theta_c|$), was 0·007°.

The density of the crystals was determined by flotation in a mixture of chloroform and tetrabromoethane, and the value obtained agreed satisfactorily with that calculated for hypoxanthine hydrochloride crystallized with one molecule of water.

Crystal data

[C$_5$N$_4$H$_5$O] Cl. H$_2$O. $M.W.=190\cdot6$.
Crystal system:

Table 1. *Final coordinates and thermal parameters with the corresponding standard deviations in parentheses*

Thermal parameters are defined by the expression:

$$T_i = \exp\left[-\tfrac{1}{4}(B_{11}h^2a^{*2} + B_{22}k^2b^{*2} + B_{33}l^2c^{*2} + 2B_{12}hka^*b^* + 2B_{13}hla^*c^* + 2B_{23}klb^*c^*)\right].$$

|	x	y	z	B_{11} or B	B_{22}	B_{33}	B_{12}	B_{13}	B_{23}
Cl⁻	1·30883 (8)	0·03147 (2)	0·22144 (4)	4·27 (2)	2·11 (1)	4·82 (2)	0·44 (1)	2·28 (1)	−0·20 (1)
O(10)	1·25413 (23)	0·40359 (7)	0·22667 (13)	3·58 (5)	2·81 (5)	4·50 (5)	−0·56 (4)	2·21 (4)	−0·69 (4)
O(6)	1·22434 (18)	0·22703 (5)	0·25773 (10)	2·83 (4)	2·90 (4)	2·79 (4)	0·10 (3)	1·61 (3)	−0·02 (3)
N(1)	0·97275 (23)	0·14527 (6)	0·39140 (12)	2·56 (5)	2·17 (5)	2·54 (5)	0·27 (4)	0·96 (4)	−0·16 (4)
N(3)	0·64203 (22)	0·18143 (6)	0·55674 (11)	2·35 (4)	2·45 (5)	2·40 (4)	−0·11 (4)	0·90 (4)	0·27 (4)
N(7)	0·90607 (23)	0·34968 (6)	0·41332 (12)	2·58 (5)	2·25 (4)	2·33 (4)	−0·24 (4)	0·98 (4)	0·08 (4)
N(9)	0·60298 (22)	0·31865 (6)	0·56813 (12)	2·34 (4)	2·63 (5)	2·18 (4)	0·29 (4)	1·01 (4)	−0·05 (4)
C(2)	0·78136 (27)	0·13088 (8)	0·48989 (15)	2·82 (6)	2·34 (5)	2·78 (6)	−0·19 (4)	0·89 (4)	0·29 (4)
C(4)	0·70871 (24)	0·25232 (7)	0·51731 (13)	1·87 (4)	2·44 (5)	1·84 (4)	0·03 (4)	0·49 (4)	0·00 (4)
C(5)	0·89924 (24)	0·27214 (7)	0·41983 (13)	1·98 (5)	2·26 (5)	1·81 (4)	−0·12 (4)	0·46 (4)	0·01 (4)
C(6)	1·04953 (25)	0·21646 (7)	0·34743 (13)	2·00 (5)	2·52 (5)	1·90 (5)	0·05 (4)	0·46 (4)	−0·09 (4)
C(8)	0·72726 (28)	0·37577 (8)	0·50389 (14)	2·95 (6)	2·28 (5)	2·66 (5)	0·16 (4)	0·80 (4)	−0·11 (4)
H(1)	1·0542 (34)	0·1074 (10)	0·3542 (17)	4·0 (4)					
H(2)	0·7487 (28)	0·0785 (9)	0·5072 (15)	2·8 (3)					
H(7)	1·0265 (37)	0·3747 (10)	0·3542 (19)	5·1 (4)					
H(8)	0·6975 (33)	0·4283 (9)	0·5186 (17)	3·8 (4)					
H(9)	0·4715 (33)	0·3201 (9)	0·6314 (17)	3·6 (4)					
H(10)	1·3648 (41)	0·3708 (11)	0·1850 (22)	5·8 (5)					
H(11)	1·3600 (40)	0·4396 (13)	0·2328 (20)	5·1 (5)					
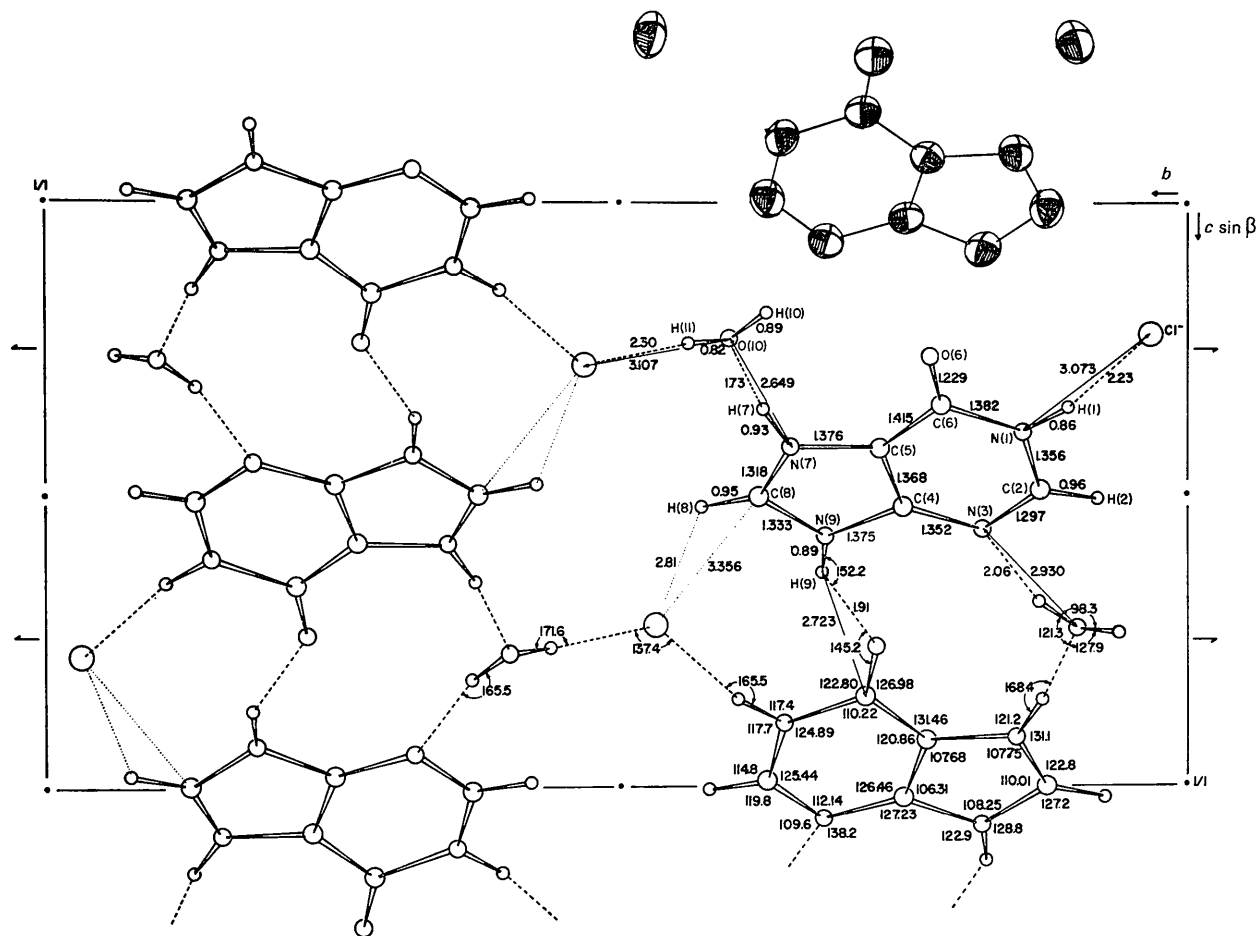
Fig. 1. Projection of the structure along [100].

Table 2. *Observed and calculated structure factors multiplied by* 10

The reflections with observed intensity less than the threshold value of $1.5\sigma_c$ are marked with $<$ signs.

monoclinic,

$a = 4\cdot8295(9)$ Å,
$b = 17\cdot7285(22)$ Å,
$c = 9\cdot0077(21)$ Å,
$\beta = 94\cdot59(3)°$.
$V = 768\cdot76$ Å^3, $F_{000} = 392$, $Z = 4$.
$D_x = 1\cdot647$ g.cm^{-3}, $D_m = 1\cdot638$ g.cm^{-3}.
Linear absorption coefficient: $\mu = 4\cdot65$ cm^{-1}.

Space group $P2_1/c$,

($h0l$ absent for $l = 2n + 1$;
$0k0$ absent for $k = 2n + 1$).
λ(Mo $K\alpha$) = $0\cdot71069$ Å.

Data were collected on a manually operated four-circle diffractometer with niobium filtered Mo $K\alpha$ radiation. The crystal used had dimensions $0\cdot5$ mm × $0\cdot3$ mm × $0\cdot2$ mm, and was mounted along [$10\bar{2}$] which approximately coincides with the needle axis. Integrated intensities were measured by the $\omega/2\theta$ scan technique, the scan ranges being calculated as $\Delta2\theta = A + B$ $\tan2\theta$ (Alexander & Smith, 1964). Suitable scan ranges for reflections with $2\theta > 12°$ were obtained with $A = 1\cdot6°$ and $B = 1\cdot0°$. The scan ranges of the low angle reflections ($2\theta < 12°$) were determined individually because the Nb K absorption edge is close to the Mo $K\alpha$ peak.

Backgrounds were measured at the beginning and end of the 2θ scan, counting each background for half the scan time. The net count was derived by subtracting the background counts from the peak counts.

Of the 1769 reflections measured within a sphere limited at sin $\theta/\lambda = 0\cdot65$, 169 were coded as unobserved, being less than the threshold value of $1\cdot5\sigma_c$, where $\sigma_c = (N_{BgI} + N_{Pk} + N_{BgII})^{1/2}$. N_{Pk} is the scan counts and N_{BgI} and N_{BgII} are the background counts. The error in the net intensity of each reflection was derived as $\sigma_I = [\sigma_c^2 + (0\cdot01\ \sigma_c^2)^2]^{1/2}$. The instability factor, $0\cdot01$ in the equation above, was estimated by plotting the fluctuation in the intensities of three standard reflections which were measured every four hours throughout the data collection.

The data were processed in the usual way and corrected for Lorentz and polarization effects and for coincidence loss (Sletten, Sletten & Jensen, 1969). The apparent deadtime for the counting system was

found to be $4\cdot35 \times 10^{-6}$ sec.count^{-1}. Absorption corrections were not made since the linear absorption coefficient is low and the crystal is roughly equidimensional.

Structure determination and refinement

The structure was solved by the heavy atom method. A structure factor calculation based on the chloride ion gave $R = 0\cdot592$ ($R = \Sigma\ ||F_o| - |F_c||/\ \Sigma\ |F_o|$). In the corresponding Fourier synthesis all the nonhydrogen atoms appeared, although close to the hypoxanthine moiety there were several additional peaks of electron densities as high as the carbon and nitrogen atoms in the ring. In the next Fourier synthesis based on the contribution from all the nonhydrogen atoms ($R = 0\cdot316$), these false peaks had disappeared.

Two cycles of full-matrix least-squares refinement, in which all the atoms were given isotropic temperature factors, decreased R to $0\cdot164$. All atoms were assigned anisotropic thermal parameters in the succeeding cycle and R decreased to $0\cdot065$. In a difference synthesis calculated at this stage, the seven hydrogen atoms were nicely resolved, and they were included in the refinement with isotropic temperature factors.

It was noticed that the calculated structure factor of reflection [112] was higher than the observed value by about 40%. This reflection had by far the highest intensity in the data set and evidently suffers secondary extinction. Accordingly, the reflection was coded extinct in the further refinement. Three cycles of refinement, including all atoms, brought R to $0\cdot030$; an additional final cycle gave no significant changes in positional or thermal parameters.

The function minimized in the refinement was $\Sigma\ w(|F_o| - (1/k)|F_c|)^2$ where $w = 1/\sigma_F^2$, σ_F being the standard deviation in the structure factors: $\sigma_F = [F^2 + \sigma_I(Lp)^{-1}]^{1/2} - F$. In the final cycle the weighted residual error $R_w = [\ \Sigma(w|F_o| - |F_c|)^2/\ \Sigma w|F_o|^2]^{1/2}$ was $0\cdot033$, and the standard deviation of an observation of unit weight [$\Sigma w(|F_o| - |F_c|)^2/(m - n)]^{1/2}$ was $2\cdot60$. All shifts in parameters were less than $0\cdot2\sigma$.

Reflections coded unobserved were given zero weight in the refinement if $|F_c| < |F_{min}|$. If $F_c| > |F_{min}|$, they were treated in the normal way with $\Delta F = w(|F_{min}| - |F_c|)$.

The atomic scattering factors used in the calculations were those given by Berghuis, Haanappel, Potters, Loopstra, MacGillavry & Veenendaal (1955) for the chloride ion, oxygen, nitrogen and carbon, and for hydrogen, those of Stewart, Davidson & Simpson (1965). All calculations were carried out on an IBM 7094 computer, with use of programs from the X-ray 63 system (Stewart, 1964).

Final atomic coordinates and thermal parameters together with the corresponding standard deviations are shown in Table 1. In Table 2 the observed and calculated structure factors are listed. The molecular dimensions, as calculated from the final coordinates, are given in Fig. 1.
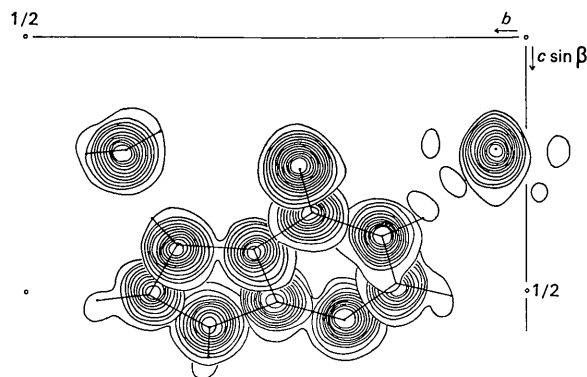

Fig. 2. Three-dimensional electron density map projected along [100]. Contours are at odd integral values of electron density for chlorine and at all integral values for the other atoms, beginning at 1 e.Å^{-3}.

A Fourier map (Fig. 2) shows relatively high electron densities for the atoms, reflecting the low temperature factors found in this structure. A difference synthesis based only on contributions from the non-hydrogen atoms was calculated (Fig. 3). In several similar structures peaks of electron density in the range 0·1–0·3 e.Å^{-3} have been observed in the center of each bond (e.g. Sletten, Sletten & Jensen, 1968, 1969). However, in this structure the only residual electron density is found in the region between atoms C(4) and C(5)

Discussion of the structure

The hypoxanthine cation

The molecular dimensions are shown in Fig. 1 and the bond lengths are listed in Table 3 together with structural data for related compounds which have been determined with comparable accuracy. Unfortunately, more than one factor varies from one tabulated structure to the other, and thus it is difficult to assert any specific influence of a substituent on the purine skeleton. A comparison between the two cations of hypoxanthine and guanine shows a remarkable agreement of the bond lengths and angles in the imidazole rings. None of the differences is larger than 1 standard deviation as given for guanine hydrochloride dihydrate (Iball & Wilson, 1965). This indicates that the amino substituent on C(2) in the guanine molecule has negligible influence on the geometry of the five-membered ring. The differences observed in the pyrimidine rings are qualitatively as predicted by LCAO–MO methods (Pullman & Pullman, 1963). A similar comparison between the dimensions in the pyrimidine rings of the positively charged hypoxanthine ion and the neutral 9-ethylhypoxanthine molecule shows small differences. Four of the bonds in the six-membered ring of the cation are significantly shorter than the corresponding bonds in the neutral molecule. The observed trend is difficult to explain in terms of possible resonance formulas.

6-Mercaptopurine as an anticarcinogenic drug is assumed to compete with hypoxanthine in the de novo synthesis of the nucleic acids, and as can be seen from Table 3 there exist only minor structural differences between the two compounds. It is most interesting to notice that the angles around carbon atom C(6) in the two molecules are identical within two standard deviations. The differences in bond lengths in the six-membered rings are in qualitative agreement with the differences in bond orders calculated by LCAO–MO methods for the neutral hypoxanthine and 6-mercaptopurine (Pullman & Pullman, 1963). Considering the rather crude approximations in the simple molecular orbital methods, it is remarkable how well the direction of structural changes caused by substituents is predicted.

Planarity of the molecule

The fused ring system of purine has always been considered as a pseudoaromatic, planar system. Any
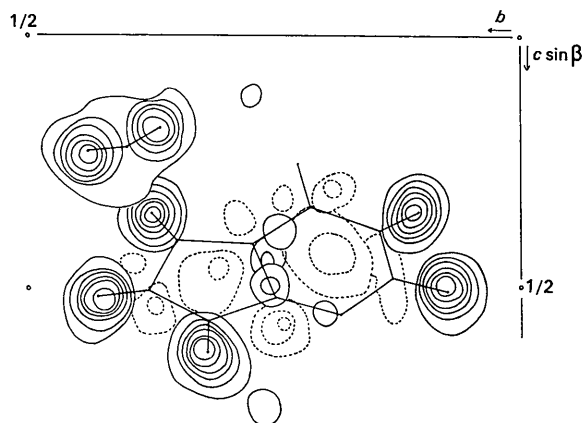

Fig. 3. Composite electron density difference map projected along [100]. Contours are at intervals of 0·1 e.Å^{-3} beginning at 0·1 e.Å^{-3}. Dashed lines show negative regions.

Table 3. Bond lengths in the hypoxanthine ion and in other purine derivatives

Approximate standard deviations in parentheses. For references see Table 4.

Bond	Hypoxanthine hydrochloride monohydrate	Guanine hydrochloride dihydrate	9-Ethyl-hypoxanthine: 5-fluorouracil	6-Mercapto-purine monohydrate	8-Azaguanine monohydrate	Purine
N(1)–C(2)	1·356 (2)	1·374 (5)	1·372	1·350 (2)	1·379 (2)	1·349 (6)
C(2)–N(3)	1·297	1·318	1·293	1·307	1·334	1·324
N(3)–C(4)	1·352	1·345	1·367	1·364	1·351	1·336
C(4)–C(5)	1·368	1·377	1·359	1·397	1·383	1·398
C(5)–C(6)	1·415	1·414	1·423	1·396	1·430	1·385
C(6)–N(1)	1·382	1·390	1·396	1·384	1·385	1·330
C(5)–N(7)	1·376	1·378	1·377	1·370	1·361	1·375
N(7)–C(8) [N(8)]	1·318	1·322	1·322	1·346	1·303	1·337
C(8)[N(8)]–N(9)	1·333	1·335	1·367	1·326	1·359	1·311
N(9)–C(4)	1·375	1·375	1·376	1·363	1·350	1·379
C(6)–O(6) [S, H]	1·229	1·237	1·239	1·676	1·224	0·93 (6)
N(1)–H	0·86 (2)	0·86	—	0·85 (2)	0·86 (2)	
C(2)–N(2) [H]	0·96	1·339	—	0·95	1·321	0·97
N(7)–H	0·93	0·93	—	0·86		0·84
C(8) [N(8)]–H	0·95	1·00	—	0·96		1·06
N(9)–H	0·89	0·85			0·90	

deviations from planarity have been ascribed to either strong hydrogen bonding or packing forces in the crystal (Macintyre, 1964). However, as more accurate structural information has been accumulated a general feature has emerged, which was not apparent in the earlier structure determination. Least-squares planes

Fig.4. Puckering of the purine rings of five compounds: (i) hypoxanthine hydrochloride monohydrate, (ii) guanine hydrochloride dihydrate, (iii) 6-mercaptopurine monohydrate, (iv) 8-azaguanine monohydrate, (v) purine.

have been calculated for the five-membered and six-membered rings for several purine derivatives (Table 4) and in all cases but one (9-ethylhypoxanthine) the purine ring is definitely bent around the C(4)–C(5) bond. This can be visualized by making a plot of the deviation from the plane of the six-membered ring as shown in Fig.4. A comparison between the root mean square deviation of the ring atoms from the plane and the mean standard deviations in positions for the same atoms shows that the five-membered rings are all planar within experimental error, while some of the six-membered rings are slightly puckered.
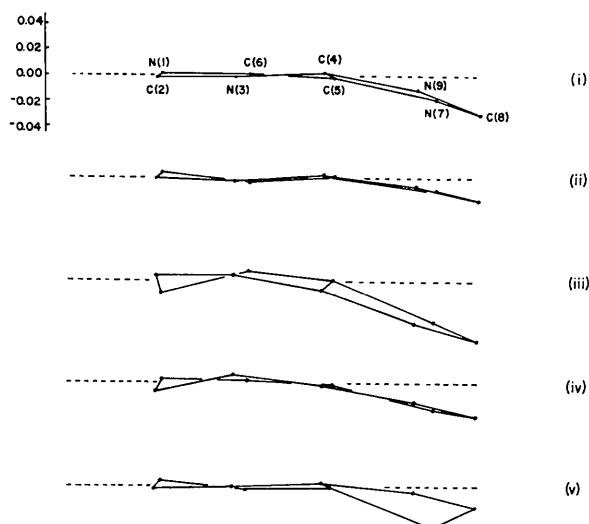
Molecular packing and hydrogen bonding

The hypoxanthine molecules, related by the c glide and a translation of one unit cell along the a axis, are linked together in ribbons by strong hydrogen bonds; O(6) (i)...H(9) (ii)–N(9) (ii), N(7) (i)–H(7) (i)...O(10) (i)–H(10) (i)...N(3) (ii) (Fig. 1). These ribbons are nearly planar and run parallel to the (102) plane. The only out of plane hydrogen bond is the water–chlorine bond interconnecting the ribbons. Ribbons connected in this way are parallel and are displaced relative to each other by approximately half a unit cell along [102]. The perpendicular distance between planes of ribbons is 3·18 Å.

In the crystalline state molecules of neutral purine derivatives are known to stack one on top of the other with an interplanar spacing in the range 3·25 Å–3·40 Å. The stacking forces are probably closely related to the

Tables 4. *Deviations of atoms from different least-squares planes, root mean square deviations from the planes of the atoms included in the calculation, standard deviations in coordinates, and angles between planes of five- and six-membered rings.*

Atoms included in calculation of planes		Hypoxanthine hydrochloride monohydrate	Guanine hydrochloride dihydrate	9-Ethyl-hypoxanthine 5-fluorouracil	6-Mercapto-purine monohydrate	8-Azaguanine monohydrate	Purine
N(1), C(2)	N(1)	0·0013	0·0035	−0·0044	0·0105	−0·0034	−0·0039
N(3), C(4)	C(2)	−0·0011	−0·0003	−0·0004	−0·0044	0·0071	0·0026
C(5), C(6)	N(3)	−0·0006	−0·0025	0·0023	−0·0045	−0·0061	0·0008
	C(4)	0·0020	0·0020	0·0009	0·0066	0·0016	−0·0027
	C(5)	−0·0017	0·0011	−0·0053	−0·0005	0·0020	0·0013
	C(6)	0·0001	−0·0037	0·0078	−0·0078	−0·0012	0·0020
	N(7)	−0·0183	−0·0202	−0·0029	0·0324	0·0199	0·0324
	C(8) or N(8)	−0·0297	−0·0367	0·0048	0·0466	0·0263	0·0157
	N(9)	−0·0111	−0·0147	0·0057	0·0333	0·0138	0·0045
	σ_{rms}	0·0018	0·0035	0·0058	0·0092	0·0059	0·0035
C(4), C(5)	C(4)	−0·0011	−0·0019	0·0005	0·0018	0·0014	0·0033
N(7), C(8) [N(8)]	C(5)	−0·0004	0·0000	−0·0002	−0·0025	0·0013	−0·0063
N(9)	N(7)	0·0019	0·0021	−0·0002	0·0024	0·0007	0·0074
	C(8) [N(8)]	−0·0027	−0·0034	0·0006	−0·0013	0·0002	−0·0057
	N(9)	0·0023	0·0033	−0·0007	−0·0004	−0·0010	0·0014
	σ_{rms}	0·0030	0·0040	0·0007	0·0040	0·0016	0·0085
	$\sigma_{x\,y\,z}$	0·0013	0·0035		0·0014	0·0013	0·004
Dihedral angles		0·79°	0·99°	0·30°	1·26°	0·68°	0·82°
References		Present paper	Iball & Wilson (1965)	Kim & Rich (1967)	Sletten, Sletten & Jensen (1969)	Sletten, Sletten & Jensen (1968)	Watson, Sweet & Marsh (1965)

degree of overlap between molecules in adjacent layers. The positively charged hypoxanthine ions are packed in a skewed 'stack' with virtually no overlap between neighboring molecules (Fig. 5). Such absence of overlap is also observed in adenine hydrochloride hemihydrate (Cochran, 1951) and in guanine hydrochloride monohydrate (Broomhead, 1951) and may reflect that repulsion between equally charged ions overrides the associative forces which are present in stacks of neutral purine moieties.

Thermal motion

The thermal motion of the atoms of this crystal is fairly low, and any correction in bond lengths because of rigid body motion would probably be negligible. The water oxygen and the chlorine ion show pronounced anisotropic thermal motion, while the thermal motion of the other atoms is approximately isotropic. The thermal ellipsoids at 50% probability are displayed in Fig. 1.
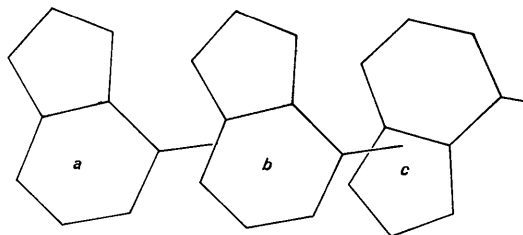
Fig. 5. Overlap between molecules in adjacent layers as viewed normal to the molecular plane. Molecules *a* and *c* are in a layer 3·18 Å below molecule *b*.

References

ALEXANDER, L. E. & SMITH, G. S. (1964). *Acta Cryst.* **17**, 1195.

BERGHUIS, J., HAANAPPEL, IJ. M., POTTERS, M., LOOPSTRA, B. O., MACGILLAVRY, C. H. & VEENENDAAL, A. L. (1955). *Acta Cryst.* **8**, 478.

BROOMHEAD, J. M. (1951). *Acta Cryst.* **4**, 92.

COCHRAN, W. (1951). *Acta Cryst.* **4**, 81.

IBALL, J. & WILSON, H. R. (1965). *Proc. Roy. Soc.* A **288**, 418.

KIM, S. H. & RICH, A. (1967). *Science,* **158**, 1046.

MACINTYRE, W. M. (1964). *Biophys. J.* **4**, 495.

PULLMAN, B. & PULLMAN, A. (1963). *Quantum Biochemistry.* Pp. 764, 779 & 791. New York: Interscience.

SLETTEN, J., SLETTEN, E. & JENSEN, L. H. (1968). *Acta Cryst.* B**25**, 1692.

SLETTEN, E., SLETTEN, J. & JENSEN, L. H. (1969). *Acta Cryst.* In the press.

STEWART, J. M. (1964). *Crystal Structure Calculations System.* Computer Sciences Center, Univ. of Maryland.

STEWART, R. F., DAVIDSON, E. R. & SIMPSON, W. T. (1965). *J. Chem. Phys.* **42**, 3175.

WATSON, D. G., SWEET, R. M. & MARSH, R. E. (1965). *Acta Cryst.* **19**, 573.

The Crystal Structure of 4-Methylthiomorpholine-1,1-dioxide

BY JOHN HERDKLOTZ AND RONALD L. SASS

Department of Chemistry, Rice University, Houston, Texas U.S.A.

The crystal structure of 4-methylthiomorpholine-1,1-dioxide has been determined by single-crystal X-ray diffraction techniques. The crystals are monoclinic, ($P2_1/c$), with $a = 11\cdot439$ Å, $b = 5\cdot88$ Å, $c = 11\cdot090$ Å, $\beta = 98\cdot56°$, $Z = 4$. A total of 814 reflections, measured above background, was collected by counter methods. The structure was refined by the method of full-matrix least-squares which led to a final weighted R index of $4\cdot1\%$ ($R = 5\cdot5\%$).

Introduction

As part of a research program on the geometry of the sulfone group in ring systems, the structure of 4-methylthiomorpholine-1,1-dioxide has been determined by single-crystal X-ray diffraction techniques.

Experimental

Crystals of 4-methylthiomorpholine-1,1-dioxide suitable for X-ray analysis were obtained from a commercial sample by slow evaporation of an anhydrous ether solution. The crystals were found to slowly sublime when exposed to the atmosphere and it was necessary to seal them in glass capillaries for all diffraction work. Crystals used in this study were prismatic in habit and averaged 0·15 mm in diameter.

On the basis of Weissenberg photographs, the systematic absences were:

$h0l$ absent for l odd,
$0k0$ absent for k odd.